

ICANS-VI

INTERNATIONAL COLLABORATION ON ADVANCED NEUTRON SOURCES

June 27 - July 2, 1982

METHODS OF NEUTRON AND PROTON DOSIMETRY AT SPALLATION SOURCES

L. R. Greenwood and R. J. Popek

Argonne National Laboratory

ABSTRACT

A variety of techniques are being developed to measure the neutron and proton fluxes and energy spectra at spallation neutron sources. Multiple-activation dosimetry is being used to adjust the neutron energy spectrum by a least-squares procedure. Primary beam protons are measured by the $^{27}\text{Al}(p,*)$ ^{22}Na reaction and secondary protons by (p,n) reactions on ^7Li , ^{51}V , and ^{65}Cu . Lithium fluoride thermoluminescent dosimeters are used to measure the neutron dose rate, although we have been unable to determine the much weaker gamma dose rate. Neutron fluxes, displacement damage, gas production and transmutation, and dose rates are now routinely determined for materials irradiations with uncertainties of 10-15%.

METHODS OF NEUTRON AND PROTON DOSIMETRY AT SPALLATION SOURCES

L. R. Greenwood and R. J. Popek
Argonne National Laboratory

1. INTRODUCTION

In order to understand radiation damage measurements at spallation neutron sources, we need to fully characterize these facilities in terms of neutron flux and energy spectra and the resultant displacement damage, transmutation, and dose rate. A companion paper at this conference¹ describes the results of such measurements² at the Radiation Effects Facility (REF) of the Intense Pulsed Neutron Source (IPNS) at Argonne National Laboratory. The present paper discusses the techniques used in these measurements.

Neutron flux and spectral measurements were made using the multiple-activation technique.³ This method has been developed for fusion material irradiations and has been successfully applied in a wide variety of neutron sources including fission reactors, 14 MeV T(d,n) sources, and Be(d,n) sources.⁴ This method measures activation products induced simultaneously in a number of materials. These integral activities are chosen to span all neutron energy regions of interest. Each integral is equal to the neutron flux-spectrum times the activation cross section. The flux-spectrum is then adjusted to obtain the best fit to the integral measurements. The final neutron spectrum is then used to calculate damage parameters. This can be done routinely with integral uncertainties of $\pm 10 - 15\%$.

2. NEUTRON FLUX AND SPECTRAL MEASUREMENTS

In order to obtain the best analysis of the IPNS neutron spectrum, more than 30 different activation products were measured using Ge(Li) gamma spectrometry. Twenty-eight reactions were used to adjust the neutron flux

spectrum.¹ The starting spectrum was calculated with the HETC⁵ and VIM⁶ computer codes. The spectral adjustment was performed with the STAYSL computer code.⁷ In this technique uncertainties and covariances are assigned to the integral activities, activation cross sections, and starting spectrum. A simultaneous least-squares adjustment is then made to all of the data. Cross sections were taken from ENDF/B-V⁸ and extended to 44 MeV⁹ using available data and calculations.

The resultant flux spectra are shown in Figures 1 and 2. Figure 1 shows the spectrum for the REF (VT2) and Figure 2 compares spectra for the REF and NSF targets. This latter difference is due to the moderators, Pb for the REF and C-Be for the NSF. These data are summarized in Table I. Flux gradients were also measured, as discussed in reference 1. Typical gradients are shown in Figures 3 and 4. Clearly, dosimetry is probably required in most materials experiments to precisely locate samples in the rather steep flux and spectral gradients.

Table I. Neutron Fluxes at IPNS
Neutrons/m²-proton (400 MeV)

Energy, MeV	REF (VT2)	NSF (H2)
Total	218	194
>0.1 MeV	151	55
Thermal	1.2	44
<1	157	180
1-5	51	10.8
5-10	4.4	1.04
10-20	1.54	0.45
>20	4.0	1.3

Several problems were considered which might interfere with this technique. First of all, if protons are present as well as neutrons, then confusion is possible as to the source of reaction products. For example, a (p,d) reaction is indistinguishable from a (n,2n) reaction. Fortunately, the proton flux is quite low, as discussed in section 4. Hence, proton interference is generally less than 1%. Secondly, our present activation cross sections do not extend above 44 MeV. This high energy flux can be neglected for all of the reactions we have used since both the cross sections and fluxes are very weak above 44 MeV. The only exception to this rule is that we apparently see interference with (n, α) reactions from high-energy spallation products. Activation rates from ^{54}Fe , ^{63}Cu , and ^{60}Co were all much higher than expected (40-80%). The most likely explanation is that the activation products can also be produced by spallation from the neglected high-energy neutrons. As proof of this we note that the worst cases appear to be those elements which have the least abundant isotopes (i.e., ^{54}Fe (n, α) may be overshadowed by ^{56}Fe spallation).

On the other hand, spallation cross sections could be extremely valuable in defining the neutron spectrum above 30 MeV. J. Routti and J. Sandberg have recently demonstrated this technique using spallation products from copper.¹⁰ We have observed these spallation products in many of our materials and plan to develop this technique, although the cross sections are not very well known. In general, neutron cross sections are very poorly known above 20 MeV, a fact which hampers neutronic and shielding calculations as well as dosimetry.

3. PROTON BEAM DOSIMETRY

The $^{27}\text{Al}(p,*)^{22}\text{Na}$ reaction has been used to monitor the direct proton beam. Originally this was done to measure beam profiles and currents. However, with improvements in the beam monitoring system we are now able to study the cross section. The measurements were performed by placing a stack of three Al foils (5 mils thick, 4" by 4" square) directly in the proton beam. The center foil was then gamma counted, the others being used to correct for recoil losses. We have focused on ^{22}Na since we want a long-lived monitor for irradiations lasting a week or more. Thus, ^{24}Na is too short-lived. We also measure ^7Be ; however, the data has not been repeatable, possibly due to the longer recoil ranges of ^7Be ions compared to those for ^{22}Na .

The results of several measurements are listed in Table II. As can be seen the ^{22}Na results are quite consistently lower than measurements with the toroids and faraday cup. The ^{22}Na yield was taken from a French evaluation.¹¹ Our results indicate that the most likely cross section at 400 MeV is 13.4 mb ($\pm 10\%$), considerably lower than the recommended value of 17.8 mb.

Table II. $^{27}\text{Al}(p,*)^{22}\text{Na}$ Cross Section Measurements

Date	Proton Energy = 400 MeV		Ratio ($^{22}\text{Na}/\text{Toroid}$)
	Previous Cross Section = 17.8 mb		
	Protons, $\times 10^{17}$		
	^{22}Na	Toroid	
11-16-81	1.20	1.63	0.74
11-20-81	1.32	1.72	0.77
02-08-82	16.4	21.9	0.75
	Average = 0.75		
Adjusted cross section = <u>13.4 mb</u> ($\pm 10\%$)			

4. SECONDARY PROTON DOSIMETRY

As mentioned previously, some concern was raised over the possibility of protons interfering with neutron dosimetry measurements. Another more serious concern is that low energy protons may deposit very high energy losses in insulators under study for radiation damage. The following measurements show that neither of these effects are significant.

In order to measure secondary proton fluxes, several materials were irradiated to look for (p,n) reactions. The $^{65}\text{Cu}(p,n)^{65}\text{Zn}$ and $^{51}\text{V}(p,n)^{51}\text{Cr}$ reactions gave the best results, mainly since neither target has any strong neutron-activation products, except from spallation. The $^{56}\text{Fe}(n,p)^{56}\text{Co}$ reaction is overwhelmed by neutron activities. Lithium fluoride was also tried; however, ^7Be from the $^7\text{Li}(p,n)$ reaction appears to be weaker than the ^7Be produced by spallation in fluorine. The Cu and V results are listed in Table III.

Table III. Secondary Proton Dosimetry
REF-VT2-400 MeV
Pb Absorption Result $\langle E \rangle \approx 100$ MeV

<u>Reaction</u>	<u>Rate/μC</u> ($\times 10^{-18}$)	<u>σ, mb</u>	<u>Flux/$\text{cm}^2\text{-}\mu\text{C}$</u> ($\times 10^8$)
$^{51}\text{V}(p,n)^{51}\text{Cr}$	2.41	10-20	≈ 1.6
$^{65}\text{Cu}(p,n)^{65}\text{Zn}$	2.50	10-20	≈ 1.7
$^{58}\text{Ni}(n,p)^{58}\text{Co}$	5493.	40.8	1346.

Secondary protons/neutrons $\approx 1/800$

Flux at 10 μA : neutrons: 1.3×10^{12} n/ $\text{cm}^2\text{-s}$
protons: $\approx 1.6 \times 10^9$ p/ $\text{cm}^2\text{-s}$

Since these two reactions have very similar thresholds and cross section values, little can be deduced about proton fluxes or energies. Another experiment was thus performed where the Cu and V samples were embedded at 16 locations in a lead cylinder measuring 1-7/8" in diameter by 3" long. Although these samples are still being analyzed, preliminary results indicate a rather even distribution of ^{65}Zn . This implies that the protons must have rather high energies, certainly above 100 MeV and more likely 150-200 MeV. The even distribution is then explained since the decrease in proton flux across the cylinder is balanced by the increase in cross section as the protons lose energy. Each of these effects is roughly a factor of two for our experimental geometry.

Since we know that the protons must have an average energy above 100 MeV, then the (p,n) activation cross sections must be in the 10-20 mb range (although neither reaction is well-known at 100-200 MeV). The proton flux must thus be about 1.6×10^8 protons/cm²- μC or about 1.6×10^9 protons/cm²-s at 10 μA beam current. This secondary proton flux is only about 1/800 of the neutron flux, as shown in Table III. These measurements are still in progress and we hope to refine our knowledge of the secondary proton flux. In any case, the present results indicate that these protons are of little concern to radiation damage and dosimetry measurements. The most likely explanation for these particles is that we are seeing protons elastically or inelastically scattered from the target and that these nearly 400 MeV protons lose about 200 MeV in the uranium target and lead moderator before we detect them.

5. DOSE MEASUREMENTS

Insulator irradiations now being done for the fusion materials program require knowledge of the total dose deposited in the samples. This dose is primarily due to neutrons, but may be weakly influenced by gammas, protons, or other charged particles. Thermoluminescent dosimeters (LiF-TLD700) were irradiated in an attempt to more accurately determine dose rates. These dosimeters were calibrated at known ^{226}Ra and ^{60}Co sources prior to their use at IPNS. The samples were irradiated in polyethelene tubing.

Nickel wires were also irradiated to determine the neutron flux using the $^{58}\text{Ni}(n,p)^{58}\text{Co}$ reaction. In order not to saturate the dosimeters it was necessary to reduce the IPNS beam-cycling rate to 1 hertz (normally 30 hz) and to expose the samples for only 1-15 minutes.

The TLD results are listed in Table IV along with background gamma

Table IV. Dose Measurements at IPNS
LiF - TLD 700
 $E_p = 400 \text{ MeV}; 1 \text{ Hz}; \sim 7 \times 10^{13} \text{ P}$

Location (REF)	Dose (Rads/ μC)	
	Exp. ($\pm 10\%$)	Calc. (neutron) ($\pm 15\%$)
VT2	18.7	19.1
VT1	17.0	18.1

<u>Background Gamma Dose</u>		
Run Time (m)	Gamma Dose, R/hr ($\pm 10\%$)	
	Pre-Run	Post-Run
1	77	92
15	82	150

doses before and after short irradiations at reduced (1/30) beam power. The calculated doses (neutron only) were determined by averaging ${}^7\text{Li}$ and F Kerma factors¹² over our measured neutron spectra, normalized to the ${}^{58}\text{Ni}(n,p)$ activation rate. As can be seen, the calculations overpredict the measured rates, although values agree within the estimated errors. One possible source of this overprediction is that the kerma factors include the full beta-particle energies even though our samples (1 mm OD by 6 mm long) will not stop all of the betas. We estimate that this effect might reduce our calculated values by as much as 10%, although more exact calculations have not been performed. In any case, it would appear that most of the dose seen in the TLD's is due to neutrons. Estimates of the gamma flux¹³ suggest that the gamma dose should be no more than 10-20% of the neutron dose and we have already shown that secondary protons are negligible. Nevertheless, it would appear that TLD measurements and calculations are not sufficiently accurate at present to really measure the weaker gamma dose and other techniques may be needed.

6. CONCLUSIONS

Techniques have been developed to characterize neutron and proton fluxes and energy spectra at spallation neutron sources. Routine neutron measurements are now being performed to provide materials experimenters with exposure data including calculated displacement, transmutation, and dose rates. These integral parameters can generally be determined to $\pm 10-15\%$ accuracy, although some problems remain. In particular, nuclear cross sections need further development above 20 MeV. Spallation cross sections (e.g., for Cu) would be especially useful and might allow us to extend the spectral adjustment technique up to the proton beam energy. Further work is also needed to measure the gamma flux at spallation sources. The use of TLD's

is questionable for this purpose due to uncertainties in the measurements and calculations. Proton dosimetry also could be improved with more nuclear reactions and better dosimetry. Work is continuing in all of these areas, although we feel that the IPNS is now sufficiently well-characterized for routine materials experiments.

REFERENCES

1. R. C. Birtcher, M. A. Kirk, T. H. Blewitt, and L. R. Greenwood, Measurement of Neutron Spectra and Fluxes at the IPNS Radiation Effects Facility, proceedings of this conference.
2. M. A. Kirk, R. C. Birtcher, T. H. Blewitt, L. R. Greenwood, R. J. Popek, and R. R. Heinrich, J. Nucl. Mater. 96, (1981) 37.
3. L. R. Greenwood, Review of Source Characterization for Fusion Materials Irradiations, BNL-NCS-51245, (1980) 75.
4. L. R. Greenwood, R. R. Heinrich, M. J. Saltmarch, and C. B. Fulmer, Nucl. Sci. Eng. 72, (1979) 175.
5. K. C. Chandler and T. W. Armstrong, Oak Ridge National Laboratory Report, ORNL-4744 (1972).
6. F. M. Gelbard and R. E. Prael, Argonne National Laboratory Report, ANL-75-2 (1974).
7. F. G. Perey, Least-Squares Dosimetry Unfolding: The Program STAYSL, ORNL-TM-6062 (1977); modified by L. R. Greenwood (1979).
8. Evaluated Nuclear Data File, Part B, Version V, National Neutron Cross-Section Center, Brookhaven National Laboratory (1979).
9. L. R. Greenwood, "Extrapolated Neutron Activation Cross-Sections for Dosimetry to 44 MeV", ANL-FPP-TM-115 (1979).

10. J. T. Routti and J. V. Sandberg, *Computer Physics Communications* 21, (1980) 119.
11. J. Tobailem, C. H. Lassus-St. Genies, and L. Leveque, CEA Report-N-1446 (1971).
12. M. A. Abdou, Y. Gohar, and R. Q. Wright, MACK-IV; A Program to Calculate Nuclear Response Functions from Data in ENDF/B Format, Argonne National Laboratory Report, ANL-FPP-77-5 (1978).
13. M. Kimura, J. M. Carpenter, and D. F. R. Mildner, Calculations of the Heat Deposition and the Expected Rate of Temperature Rise in Moderator, Reflector, and Decoupler Materials at IPNS-I, Argonne National Laboratory Report, ANL-81-22 (1981).

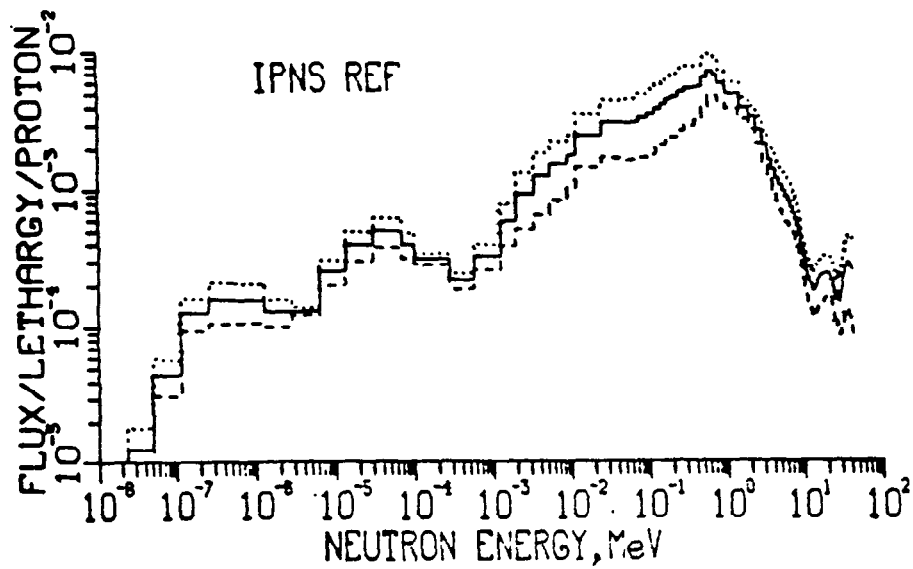


Figure 1. Neutron spectrum unfolded at the Intense Pulsed Neutron Source. The dotted and dashed lines represent one standard deviation. At least 28 activation reactions were measured. The spectrum extends to 500 MeV (not shown).

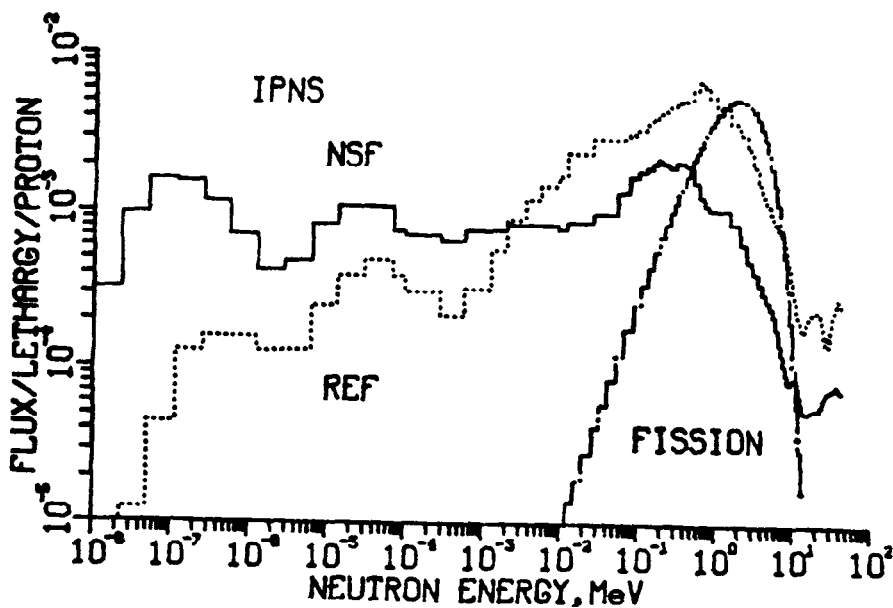


Figure 2. Comparison of neutron spectra at the Radiation Effects Facility (Pb moderator), the Neutron Scattering Facility (C-Be moderator), and a pure fission spectrum.

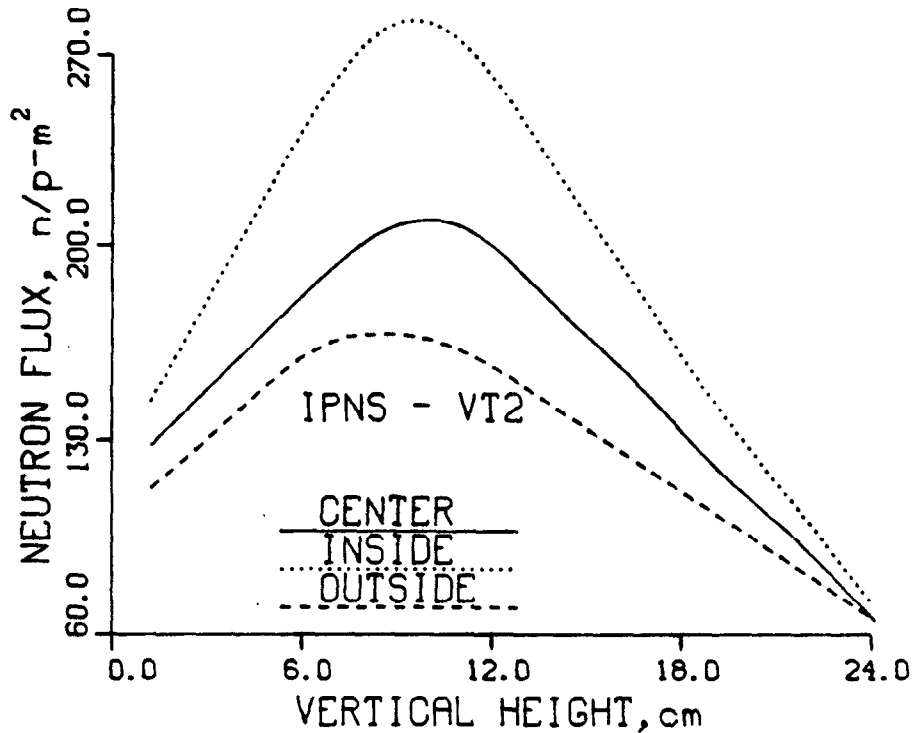


Figure 3. Vertical flux gradients in the vertical thimble 2 of IPNS-REF. The solid line was at the center of the tube; the dotted line was on the inside radius, 2 cm closer to the target; the dashed line was on the outside radius, 2 cm farther from the target.

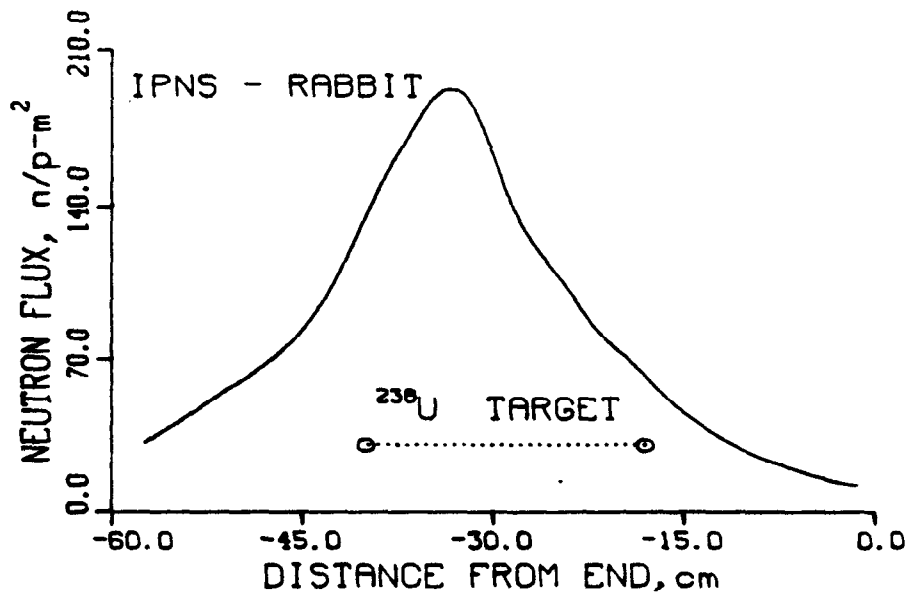


Figure 4. Horizontal flux gradients measured in the center of the IPNS-REF rabbit tube, parallel to the ^{238}U target. Distances are relative to the end of the rabbit hole. The target location is shown. The beam is incident from the left.